Journal of Inflammation

RESEARCH

Open Access

Exosomes derived from M2 macrophages regulate airway inflammation by modulating epithelial cell proliferation and apoptosis

Yinying Ren[1], Mi Zhou[1], Yuehan Li[1], Yan Li[1], JinYing Xiang[1], Fang Deng[1], Zhengxiu Luo[1], Enmei Liu[1], Jinyue Yu[2,3], Zhou Fu[1], Fengxia Ding[1*] and Bo Liu[4*]

Abstract

Background Asthma is a chronic inflammatory disease characterized by airway remodeling and immune dysregulation. This study aimed to explore the mechanisms by which M2 macrophage-derived exosomes (M2Φ-Exos) regulate airway inflammation in asthma by modulating epithelial cell proliferation and apoptosis.

Methods M2Φ-Exos were extracted and characterized by morphology, size, and marker protein expression. In vitro, the effects of M2Φ-Exos on House Dust Mites (HDM)-stimulated mouse lung epithelial cells (MLE-12s) were evaluated using western blotting to analyze Proliferating Cell Nuclear Antigen (PCNA), B-cell lymphoma-2 (Bcl-2), Bcl-2-associated X protein (Bax), and cleaved caspase-3 expression. In vivo, M2Φ-Exos were administered to HDM-induced asthmatic mice to assess their impact on airway inflammation, epithelial remodeling, and proliferation-apoptosis balance using immunohistochemistry, immunofluorescence, and western blotting. Cytokine levels in lung tissue and bronchoalveolar lavage fluid (BALF) were measured by qRT-PCR and ELISA.

Results M2Φ-Exos displayed typical cup-shaped morphology, an average diameter of 115.5 nm, and expressed marker proteins CD9, TSG101, and CD63. MLE-12 cells internalized M2Φ-Exos, leading to reduced abnormal proliferation and apoptosis in HDM-stimulated cells. In asthmatic mice, M2Φ-Exos alleviated airway inflammation and epithelial thickening while reducing PCNA, cleaved caspase-3, and Bax levels and increasing Bcl-2 expression. M2Φ-Exos suppressed pro-inflammatory cytokines (IL-4, IL-5, IL-13) and Transforming growth factor (TGF)-β, while enhancing anti-inflammatory cytokine IFN-γ and IL-10.

Conclusion These findings demonstrate that M2Φ-Exos regulate the imbalance in epithelial proliferation and apoptosis in asthma, reducing inflammation and mitigating tissue remodeling, and provide new insights into potential therapeutic strategies for asthma management.

Keywords Asthma, Proliferation, Apoptosis, M2 macrophage, Exosome

*Correspondence:
Fengxia Ding
482613@hospital.cqmu.edu.cn
Bo Liu
lbcqmu@126.com

Full list of author information is available at the end of the article

Introduction

Asthma is a prevalent and complex heterogeneous disease characterized by chronic airway inflammation, airway remodeling, and variable expiratory airflow limitation [1]. Its prevalence is rising globally, particularly among children, posing significant challenges to public health [2]. For children, asthma disrupts daily life, hampers academic performance, and imposes an immense emotional and financial burden on families and communities [3]. Although inhaled corticosteroids (ICS) and long-acting beta2-agonists (LABAs) are effective for managing recurrent asthma symptoms, a subset of patients remains poorly controlled despite optimized therapy [4]. This underscores the urgent need to identify novel, targeted therapeutic approaches for asthma management.

The airway epithelium plays a central role as both a structural and immunological barrier, serving as the first line of defense against allergens, pathogens, and environmental pollutants [5]. Dysfunction of airway epithelial cells (AECs) disrupts the epithelial barrier, leading to abnormal cytokine secretion and activation of immune responses, which are critical in asthma pathogenesis [6]. Repair of damaged AECs involves processes such as proliferation, migration, apoptosis, and differentiation. However, in asthma, this repair process is often impaired, contributing to airway remodeling and disease progression [7]. For example, in severe asthma, bronchial epithelial cells exhibit hyperproliferation, which correlates with epithelial thickness and disease severity [8]. Proliferating cell nuclear antigen (PCNA), a key regulator of DNA replication and repair, is upregulated during epithelial cell proliferation and has been implicated in the pathophysiology of asthma. Studies have demonstrated that PCNA expression is elevated in corticosteroid-dependent asthma and correlates with airway epithelial thickening, highlighting its role in airway remodeling [9].

In addition to proliferation, epithelial cell apoptosis is another critical contributor to asthma pathogenesis [10]. Dysregulated apoptosis of AECs exacerbates airway damage and perpetuates chronic inflammation. Evidence from both animal and human studies has shown increased apoptosis in AECs during asthma, driven by heightened expression of apoptotic markers such as caspase-3and pro-inflammatory cytokines associated with Th2 and eosinophilic inflammation [11]. Allergen exposure, such as house dust mites (HDM) or fungal allergens, further elevates reactive oxygen species (ROS) and apoptosis in pulmonary epithelial cells, aggravating airway inflammation [12]. Additionally, reduced expression of SIRT3 in bronchial tissues has been linked to increased epithelial apoptosis and worsened airway inflammation in asthma models [13]. These findings emphasize that targeting epithelial apoptosis could provide a novel therapeutic avenue for asthma treatment.

Exosomes, nanoscale extracellular vesicles (50–150 nm), have emerged as promising mediators in intercellular communication and potential therapeutic tools. These vesicles carry diverse bioactive molecules, including proteins, lipids, mtDNA, mRNA, and non-coding RNAs, enabling their involvement in numerous physiological and pathological processes [14, 15]. Notably, exosomes have demonstrated therapeutic effects in various lung diseases, including asthma [16], due to their low immunogenicity, biocompatibility, and ability to serve as engineered delivery vehicles. Macrophages, a key player in immune modulation, can differentiate into M1 (pro-inflammatory) and M2 (anti-inflammatory) phenotypes depending on external stimuli [17]. M1 macrophages are characterized by elevated surface expression of co-stimulatory molecules (CD80, CD86) and pro-inflammatory cytokines including interleukin-1 beta (IL-1β) and tumor necrosis factor-alpha (TNF-α). In contrast, M2 macrophages exhibit distinct molecular signatures, including upregulation of arginase-1 (Arg1), Mannose receptor C-type 1 (MRC1/CD206), Chitinase-like protein 3 (Ym1/Chil3) [18]. M2 macrophages (M2Φ) exhibit anti-inflammatory properties, promote tissue repair, and regulate immune responses [19]. Recent studies have highlighted the therapeutic potential of M2 macrophage-derived exosomes (M2Φ-Exos). For instance, M2Φ-Exos have been shown to accelerate diabetic fracture healing by promoting the M1-to-M2 macrophage transition [20]. They have also demonstrated efficacy in modulating odontogenic differentiation, neurogenesis, and angiogenesis in regenerative therapies [21]. Furthermore, M2Φ-Exos can inhibit polymorphonuclear neutrophil migration and NET formation, mitigating lung injury and reducing sepsis-related mortality [22]. These findings suggest that M2Φ-Exos may represent a promising therapeutic avenue for diseases involving immune dysregulation.

Despite these advancements, the role of M2Φ-Exos in regulating epithelial cell proliferation and apoptosis in asthma remains largely unexplored. In this study, we isolated M2Φ-Exos and evaluated their effects on HDM-induced asthma models both in vivo and in vitro. Our findings reveal that M2Φ-Exos effectively modulate airway inflammation and protect against AEC damage by reducing apoptosis and abnormal proliferation. Furthermore, our findings suggest that M2Φ-Exos may contribute to airway repair processes and modulate airway

remodeling, indicating potential therapeutic value for asthma.

Materials and methods

Ethical approval

All experimental procedures were reviewed and approved by the Ethics Committee of the Children's Hospital of Chongqing Medical University (Approval Numbers: 0918001). Animal studies were performed in compliance with the institutional guidelines for the care and use of laboratory animals and adhered to the ethical standards outlined by the Institutional Animal Care and Use Committee (IACUC).

Cell culture

Mouse alveolar macrophage cell line (MH-S) (ATCC Catalog No.: CRL-2019) and mouse lung epithelial cell line (MLE-12) (ATCC Catalog No.: CRL-2110) were obtained from the American Type Culture Collection (ATCC). MH-S cells were maintained in RPMI 1640 medium (Gibco, USA) supplemented with 10% fetal bovine serum (FBS, VivaCell, Shanghai, China), while MLE-12 cells were cultured in a complete medium (iCell, Shanghai, China). All cultures were maintained at 37 °C in a humidified incubator with 5% CO_2.

To induce M2 macrophage polarization, MH-S cells were treated with 10 ng/ml mouse interleukin-4 (IL-4; Solarbio, Beijing, China) for 48 h. MLE-12 cells were stimulated with 50 μg/ml house dust mite (HDM; Greerlabs, USA, XPB82D3A2.5) for 48 h to induce sensitization.

Serum exosome depletion by differential centrifugation

FBS (VivaCell, Shanghai, China) was transferred into sterile, ultracentrifuge-compatible tubes and carefully balanced using an analytical balance. The samples were subjected to ultracentrifugation at 120,000 × g for 12 h at 4 °C. Following centrifugation, the supernatant—containing exosome-depleted serum—was gently aspirated to avoid disturbing the exosome-containing pellet, aliquoted into sterile 50 mL tubes, and stored at − 40 °C until further use.

Extraction and characterization of exosomes

After inducing M2Φ polarization, the culture medium of MH-S cells was replaced with RPMI 1640 supplemented with 10% exosome-depleted FBS for 48 h. The medium was sequentially centrifuged at 1,000 g for 10 min and 2,000 g for 20 min to remove cell debris and apoptotic bodies. The supernatant was further centrifuged at 10,000 g for 30 min at 4 °C to eliminate larger microvesicles.The resulting supernatant was ultracentrifuged at 100,000 g for 70 min at 4 °C. The pellet was washed with Dulbecco's Phosphate Buffered Saline (D-PBS) and centrifuged again at 100,000 g for another 70 min [23, 24]. The final exosome pellet was resuspended in D-PBS and filtered through a 0.22 μm sterile pore filter.Exosome size distribution was analyzed using nanoparticle tracking analysis (NTA), while their morphology was examined using transmission electron microscopy (TEM, FEI Tecnai 12, Philips). Western blotting confirmed the expression of exosomal markers CD9, CD63, and TSG101, as well as the absence of calnexin (Zen Bioscience, Chengdu, China). Exosome protein concentration was quantified using a BCA protein assay kit (Beyotime, Shanghai, China).

Uptake of M2Φ-exos in vitro and in vivo

To evaluate the uptake of M2Φ-Exos by MLE-12 cells in vitro, exosomes were labeled with PKH26 dye following the manufacturer's instructions (Sigma, USA). After labeling, the exosomes were washed thoroughly with D-PBS and subjected to ultracentrifugation at 100,000× g for 70 min at 4 °C to remove unbound dye. The PKH26-labeled M2Φ-Exos were then resuspended in PBS and incubated with MLE-12 cells for 12 h. Subsequently, cell nuclei were counterstained with DAPI (Beyotime, Shanghai, China). Fluorescence imaging was conducted using a laser scanning confocal microscope (Nikon, Tokyo, Japan).

For in vivo tracking, firstly, total protein concentration of the M2Φ-Exos was quantified using the BCA Protein Assay Kit (Beyotime, Beijing, China). M2Φ-Exos protein concentration (2.29 μg/μl) was adjusted to 1 μg/μl with PBS prior to use. Then M2Φ-Exos were labeled with 2 μM DiR (MCE, USA) by incubation for 1 h at 37 °C, as per the manufacturer's protocol. Mice were intranasally administered 30 μg of labeled exosomes. After 24 h, the mice were euthanized, and lung tissues were analyzed using an NIR-II imaging system (Series III 900/1700, NIROPTICS, Suzhou, China).

HDM-induced allergic mouse model

Female C57BL/6 mice (6–8 weeks old, weighing 18–20 g) were procured from the Experimental Animal Center at Chongqing Medical University (Chongqing, China). All mice were maintained in a specific-pathogen-free (SPF) facility with controlled conditions, including a 12-hour light/dark cycle, 40 ± 5% relative humidity, and a temperature of 23 ± 1 °C. The animal care and experimental protocols complied with the guidelines established by the Chinese Council on Animal Care and Use.

The HDM-induced asthma model was generated based on previously reported methods [25]. HDM was

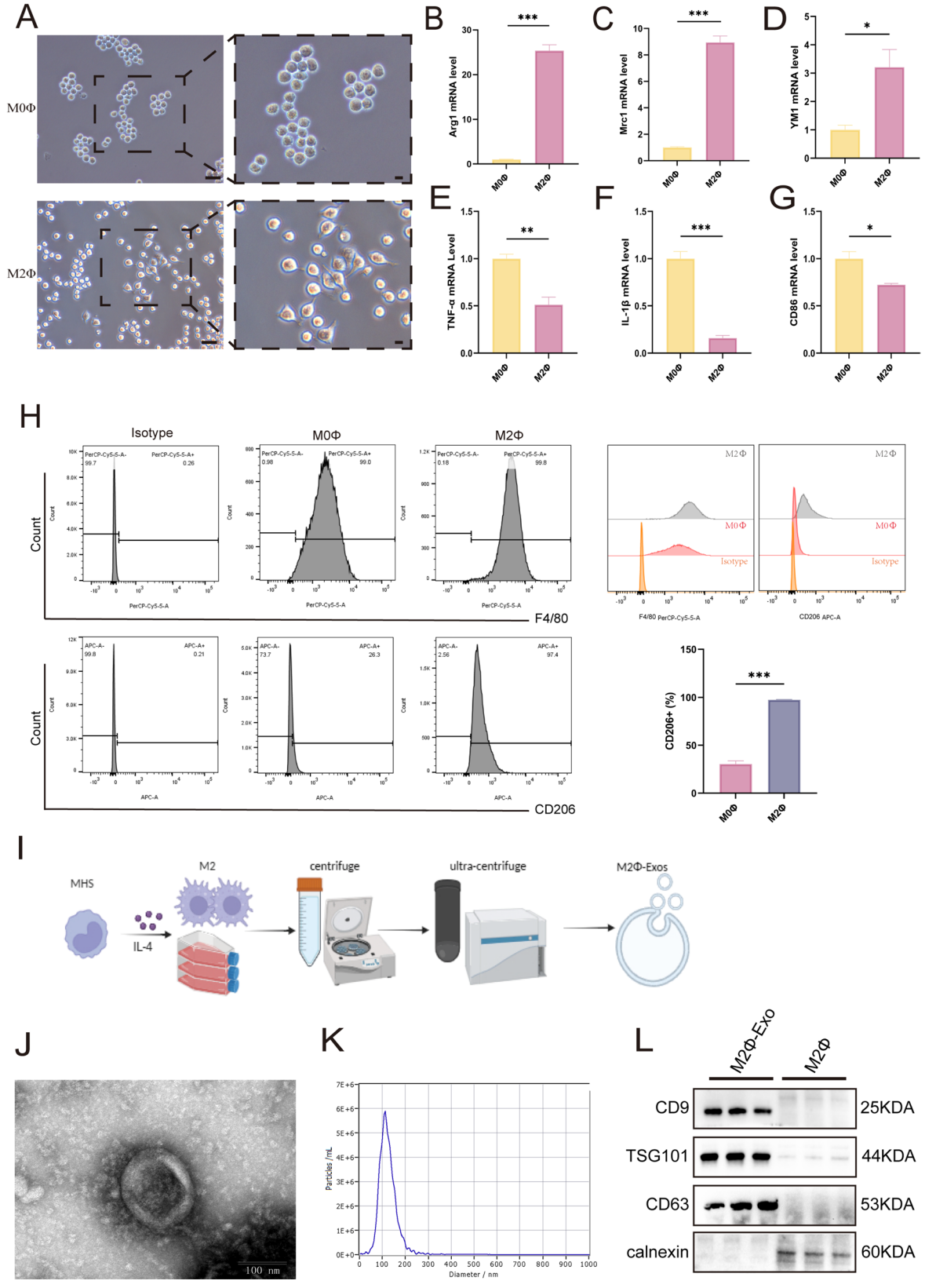

Fig. 1 (See legend on next page.)

(See figure on previous page.)

Fig. 1 Identification of M2Φ and M2Φ-Exosomes. **A** Morphological analysis of M2Φ under a microscope. Scale bar = 100 nm. **B**-**G** Gene expression of M2Φ-associated markers (Arg1, Mrc1, and YM1) and M1Φ-associated markers (TNF-α, IL-1β and CD86) quantified by RT-qPCR. **H** Expression of surface biomarkers F4/80 and CD206 on M2Φ, determined by flow cytometry. **I** Extraction process of M2Φ-derived exosomes (M2Φ-Exos). **J** Transmission electron microscopy (TEM) of exosomes isolated from the supernatant of M2Φ. Scale bar = 100 nm. **K** Size distribution of M2Φ-Exos measured by nanoparticle tracking analysis (NTA). **L** Western blot analysis of exosome marker proteins CD9, TSG101, and CD63, along with the endoplasmic reticulum marker protein Calnexin. $^{*}P < 0.05$, $^{**}P < 0.01$, $^{***}P < 0.001$

dissolved in sterile 0.9% saline to a final concentration of 0.5 μg /μl (20 μg /40μl). M2-exosomes were diluted in sterile 0.9% saline to a final concentration of 1 μg/μL(30 μg /30μl). The prepared solution was maintained on ice and utilized within 30 min to ensure exosome stability and prevent aggregation. Mice were randomly assigned to one of three groups ($n = 5$ per group): Control, Asthma, and M2Φ-Exos Treatment. Asthma was induced via intranasal administration of 20 μg HDM on days 0 and 14 for sensitization, followed by subsequent intranasal challenges with 20 μg HDM on days 21, 23, 25, 27, and 29. Control group mice received normal saline intranasally on corresponding days. Starting on day 30, the M2Φ-Exos Treatment group received 30 μg M2Φ-Exos was performed by intranasal administration (via nasal droplets using a micropipette with a 10-μl tip) for three consecutive days [26]. On day 33, all mice were euthanized for further analyses.

Bronchoalveolar lavage and cell quantification

To collect bronchoalveolar lavage fluid (BALF), the right lung of each mouse was flushed three times using cooled, sterile phosphate-buffered saline (PBS). The obtained BALF was centrifuged at 2500 rpm for 10 min to separate the cellular components. The resulting cell pellet was treated with red blood cell lysis buffer and subsequently counted using a cell counter. The supernatant was collected and stored at -80 °C for later ELISA analysis. Eosinophil counts were determined through Wright-Giemsa staining (Jiancheng Technology Co., Nanjing, China) as per the manufacturer's instructions. Eosinophil proportions were assessed by evaluating at least 200 cells, and the absolute eosinophil count was calculated accordingly [25, 27].

Histological staining and immunohistochemistry

The left lung was ligated and fixed in 4% paraformaldehyde overnight. Following fixation, 4 μm paraffin-embedded tissue sections were prepared and subjected to hematoxylin-eosin (HE) staining and immunohistochemical (IHC) analysis. The extent of inflammation in the lung tissue was assessed using a 0–3 scoring scale, as previously reported [27]. The inflammation around the bronchi, blood vessels, and pulmonary interstitium was assessed using hematoxylin and eosin (H&E) staining, and graded from 0 to 3. A score of 0 indicated no inflammatory response; 1 indicated inflammatory infiltration around the bronchi, blood vessels, and pulmonary interstitium without thickening; 2 indicated obvious inflammatory infiltration and mild thickening around the bronchi, blood vessels, and pulmonary interstitium; and 3 indicated significant inflammatory infiltration and marked thickening around the bronchi, blood vessels, and pulmonary interstitium. Collagen deposition was assessed using Masson's trichrome staining kit (Leagene Biotechnology, China) following the manufacturer's instructions. Collagen deposition was quantitatively analyzed using ImageJ. Collagen Volume Fraction (CVF) = (Blue-positive area / Total tissue area) × 100%.

IHC staining was used to evaluate the expression of PCNA and cleaved-caspase 3. Sections were incubated with primary antibodies: rabbit anti-PCNA (1:200; ProteinTech, Wuhan, China) and rabbit anti-cleaved-caspase 3 (1:200; ProteinTech, Wuhan, China). The sections were incubated with goat anti-rabbit IgG (ZSGB-BIO, Beijing, China) at room temperature for 30 min in the dark. Brown staining, indicative of positive expression, was visualized with a diaminobenzidine (DAB) solution (ZSGB-BIO, Beijing, China). The percentage of positively stained area was quantified using ImageJ software.

TUNEL assay

MLE-12 cells were fixed with 4% paraformaldehyde for 15 min, followed by permeabilization with 0.2% Triton X-100 (Solarbio, Beijing, China) for 20 min. For paraffin-embedded lung sections, deparaffinization was performed using xylene, and rehydration was carried out through a graded ethanol series. Apoptotic cells were subsequently detected using the One-step TUNEL In Situ Apoptosis Kit (Elabscience, Wuhan, China). Fluorescence images were captured using a laser scanning confocal microscope (Nikon, Tokyo, Japan).

Cell viability assay

To assess the optimal concentration of M2Φ-Exosomes (M2Φ-Exos) in MLE-12 cells, a cell counting kit-8 (CCK-8) assay was performed. MLE-12 cells were seeded into 96-well plates at a density of 4×10^3 cells per well. After a 12-hour incubation, the cells were treated with HDM, with or without M2Φ-Exos, for 48 h. Following

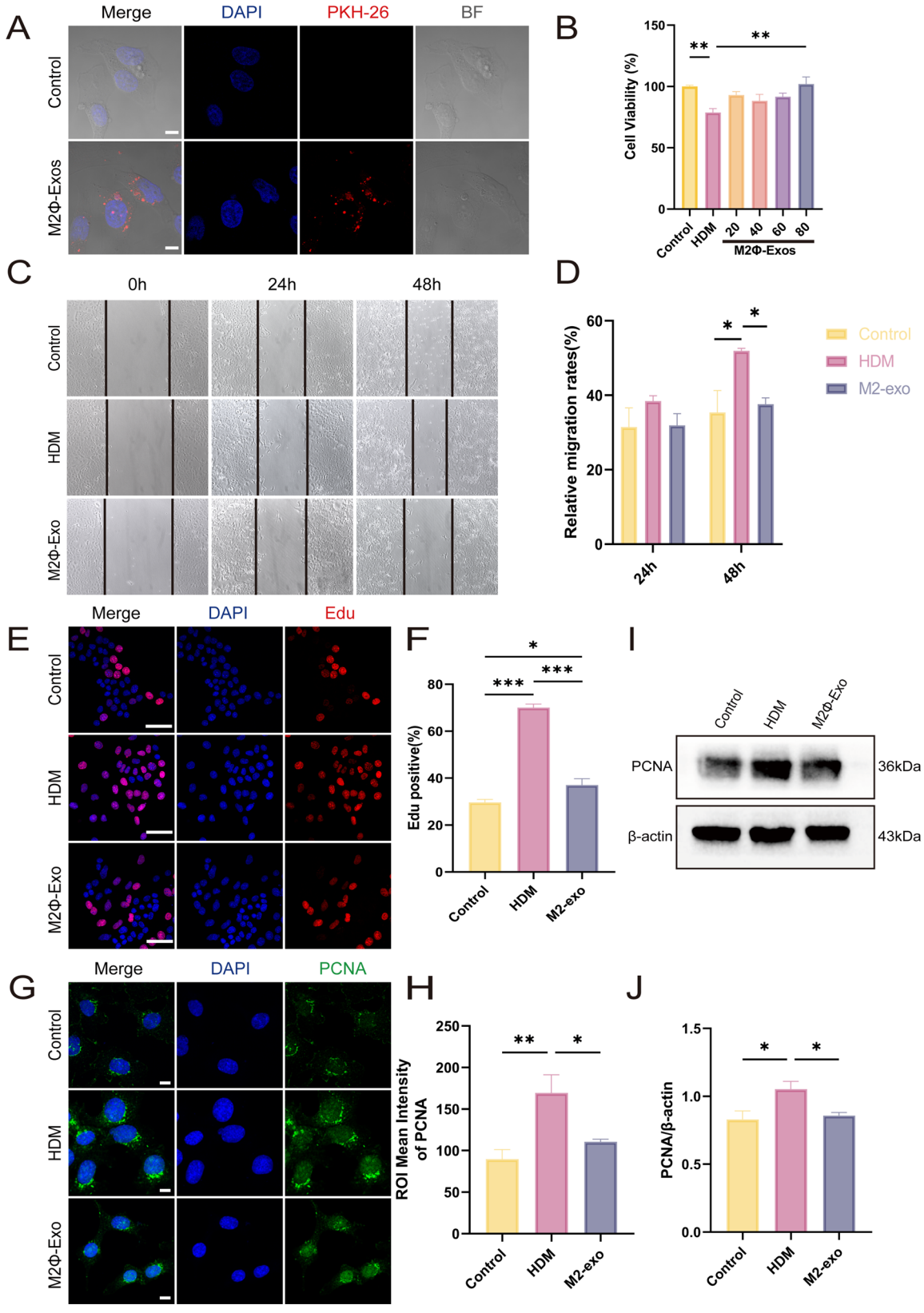

Fig. 2 (See legend on next page.)

(See figure on previous page.)

Fig. 2 M2-Exosomes inhibit the proliferation of MLE-12 cells induced by HDM. **A** Immunofluorescence staining showing the uptake of PKH-26-labeled M2Φ-Exosomes (red) by MLE-12 cells (DAPI, blue; PKH-26, red; BF, bright field). Control: untreated cells (without PKH26). Scale bar = 10 μm. **B** Cell viability of MLE-12 cells analyzed by the CCK-8 assay following treatment with varying concentrations of M2Φ-Exosomes. **C** Migration ability of MLE-12 cells assessed by wound healing assays at 24 h and 48 h post-treatment. **D** Quantitative analysis of wound healing in MLE-12 cells. **E** Proliferation of MLE-12 cells analyzed by EdU incorporation assay. Scale bar = 50 μm. **F** Quantification of EdU-positive cells. **G** Immunofluorescence staining for PCNA in MLE-12 cells. Scale bar = 10 μm. **H** Quantification of the region of interest (ROI) mean intensity of PCNA. **I** Western blot analysis of PCNA expression in the three groups. **J** Quantification of grayscale values from Western blot analysis. $^{*}P < 0.05$, $^{**}P < 0.01$, $^{***}P < 0.001$

treatment, CCK-8 solution (Beyotime, Shanghai, China) was added to each well, and the plate was incubated for an additional 2 h. Absorbance was measured using a multi-mode reader (BioTek, USA).

Wound healing assay

MLE-12 cells were seeded into 6-well plates at a density of 2×10^5 cells per well in complete culture medium and cultured until they reached 85–90% confluence. A wound was created by scratching the monolayer using a 200 μL pipette tip, and the wells were then washed twice with PBS. The culture medium, supplemented with HDM with or without M2Φ-Exosomes, was added, and FBS was excluded. Cells were incubated at 37 °C. Images of the wound area were captured at 0, 24, and 48 h using an inverted microscope, and the data were analyzed with ImageJ software.

EdU incorporation assay

Cell proliferation was assessed using the E-Click EdU Cell Proliferation Imaging Assay Kit (Elabscience, Wuhan, China) following the manufacturer's protocol. Briefly, samples were incubated with 10 μM EdU at 37 °C for 2 h. Nuclei were then stained with DAPI (Beyotime, Shanghai, China). EdU-positive cells were visualized using a laser scanning confocal microscope (Nikon, Japan), and the percentage of positive cells was determined.

Western blotting

Proteins were extracted from the right lung tissue cells of mice and MLE-12 cells according to the manufacturer's protocol (Kaige Biotechnology, Jiangsu, China). The concentration of total protein was determined using the Pierce BCA Protein Assay Kit (Beyotime, Beijing, China). Protein samples were separated by 12.5% SDS-PAGE and transferred to polyvinylidene fluoride (PVDF) membranes. After blocking with a fast blocking solution (Beyotime, Beijing, China) for 20 min at room temperature, the membranes were incubated overnight at 4 °C with primary antibodies: rabbit anti-mouse CD9 (1:1000, Zen Bioscience, Chengdu, China), CD63 (1:1000, Zen Bioscience, Chengdu, China), TSG101 (1:1000, Zen Bioscience, Chengdu, China), Calnexin (1:1000, Zen Bioscience, Chengdu, China), Bcl2 (1:500, Zen Bioscience, Chengdu, China), Bax (1:1000, Zen Bioscience, Chengdu, China), Caspase 3 (1:2000, Proteintech, Wuhan, China), Cleaved-caspase 3 (1:1000, Proteintech, Wuhan, China), PCNA (1:3000, Proteintech, Wuhan, China), and β-actin (1:10000, Zen Bioscience, Chengdu, China). The membranes were then incubated with HRP-conjugated goat anti-rabbit IgG (1:1000, Proteintech, Wuhan, China) for 1 h at room temperature. Protein bands were detected using an ECL reagent (Zen Bioscience, Chengdu, China) and visualized with a Bio-Rad imaging system (California, USA). Protein expression was quantified using Image J software.

Quantitative real-time PCR

Total RNA was extracted from mouse lung tissue and MLE-12 cells using the RNA extraction kit (BioFLUX, China, BSC52S1) following the manufacturer's protocol. The extracted RNA was then reverse transcribed into complementary DNA (cDNA) using the Evo M-MLV Reverse Transcription Kit (Aike Rui Biotechnology, Hunan, China). Quantitative Real-Time PCR (qRT-PCR) was performed with the SYBR Green Pro Taq pre-mix kit (Aike Rui Biotechnology, Hunan, China) according to the manufacturer's guidelines. Mouse β-actin was used as an internal reference gene. The following primers were used for the target genes:

IL-4: forward 5'-GGAGATGGATGTGCCAAACG-3', reverse 5'-TGGAAGCCCTACAGACGAG-3'
IL-5: forward 5'-AGCAATGAGACGATGAGGCTT-3', reverse 5'-TACCCCCACGGACAGTTTGA-3'
IL-13: forward 5'-GTATGGAGTGTGGACCTGGC-3', reverse 5'-TTTTGGTATCGGGGAGGCTG-3'
IL-10: forward 5'-GCACTACCAAAGCCACAAGG-3', reverse 5'- TGCCAGTCAGTAAGAGCAGG-3'
IFN-γ: forward 5'-GAGGTCAACAACCCACAGGTC-3', reverse 5'-TCTTCCCCCACCCCGAATCA-3'
TGF-β: forward 5'-GTTCTTCTCAGGAGCCTCTTCAT-3', reverse 5'- TGGCTTGCTCTCACAGTCC – 3'
Arg1: forward 5'-CATTGGCTTGCGAGACGTAGAC-3', reverse 5'-GCTGAAGGTCTCTTCCATCACC-3'
Mrc1: forward 5'-GTTCACCTGGAGTGATGGTTCTC-3', reverse 5'-AGGACATGCCAGGGTCACCTTT-3'

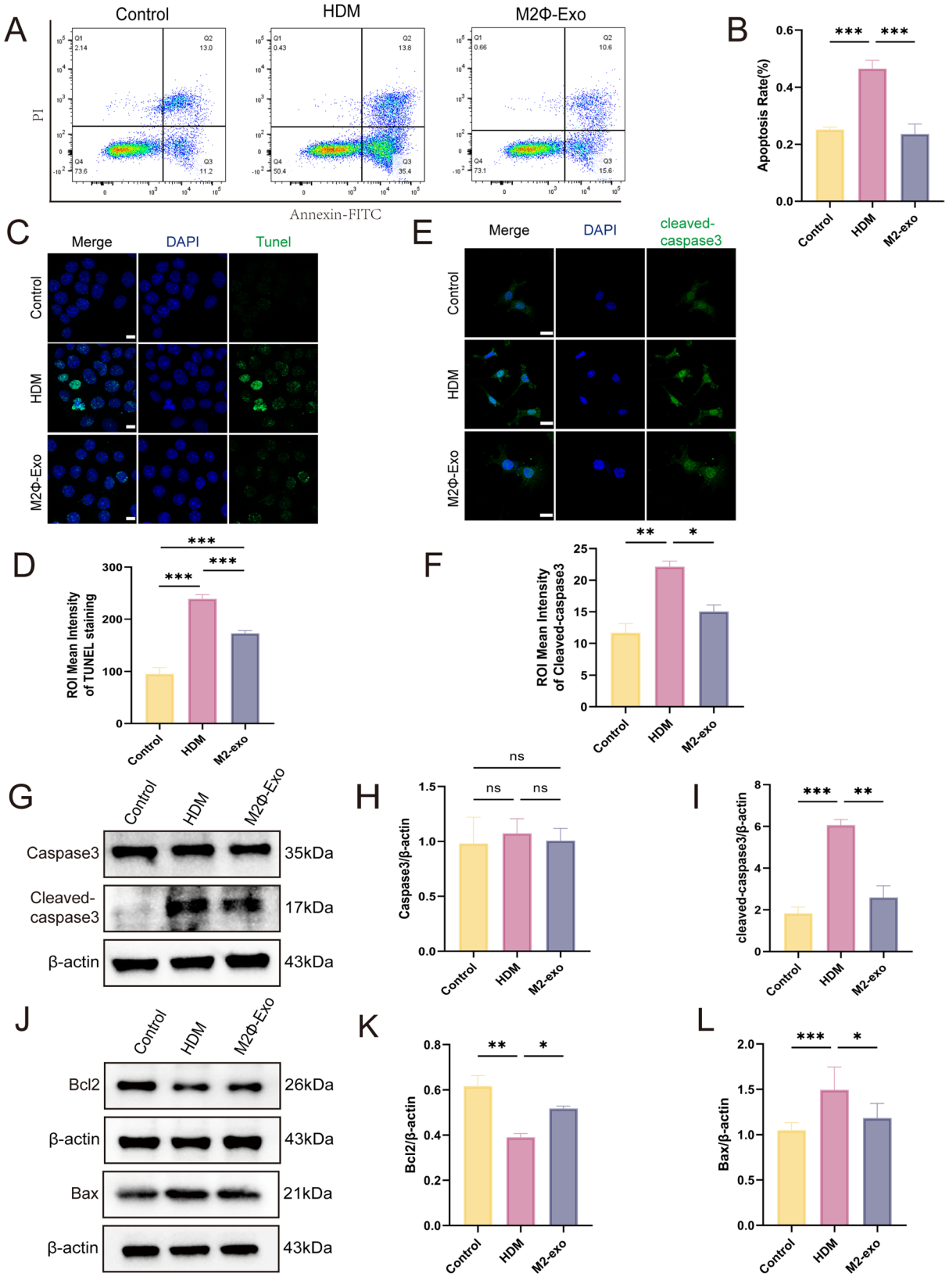

Fig. 3 (See legend on next page.)

(See figure on previous page.)

Fig. 3 M2Φ-Exosomes reduce apoptosis in MLE-12 cells induced by HDM. **A** Apoptosis of MLE-12 cells was analyzed using Annexin V-FITC/PI staining by flow cytometry. **B** Flow cytometric analysis of apoptosis in MLE-12 cells. **C** Representative immunofluorescence images of TUNEL staining in the three groups. Scale bar = 10 μm. **D** Quantification of the region of interest (ROI) mean intensity of TUNEL staining. **E** Immunofluorescence staining for Cleaved-caspase3 in MLE-12 cells. Scale bar = 20 μm. **F** Quantification of ROI mean intensity of Cleaved-caspase3. **G** Representative western blots of caspase 3 and Cleaved-caspase3 proteins, and **H**, **I** quantification of grayscale values. **J** Representative western blots of Bax and Bcl2 proteins, and **K**, **L** quantification of grayscale values. *N* = 3/group. **P* < 0.05, ***P* < 0.01, ****P* < 0.001, ns, not significant

YM1: forward
5'-TACTCACTTCCACAGGAGCAGG-3', reverse
5'-CTCCAGTGTAGCCATCCTTAGG-3'
TNF-α: forward 5'-GCTGCACTTTGGAGTGATCG-3', reverse 5'-GGGTTTGCTACAACATGGGC-3'
IL-1β: forward
5'-CCAGCTTCAAATCTCACAGCAG-3', reverse
5'-CTTCTTTGGGTATTGCTTGGGATC-3'
CD86: forward
5'-ATATGACCGTTGTGTGTGTTCTGGA-3', reverse
5'-AGGGCCACAGTAACTGAAGCTGTAA-3'
β-actin: forward
5'-GTGCTATGTTGCTCTAGACTTCG-3', reverse
5'-AGCCACAGGATTCCATACC-3'。

Immunofluorescence

Lung tissue paraffin sections and MLE-12 cells were fixed in 4% paraformaldehyde for 15 min and permeabilized with 0.2% Triton X-100 (Solarbio, Beijing, China) for 20 min. After blocking with 5% BSA (Solarbio, Beijing, China), samples were incubated overnight at 4 °C with primary antibodies: rabbit anti-mouse PCNA (1:200, ProteinTech, Wuhan, China) and rabbit anti-Cleaved-caspase 3 (1:100, ProteinTech, Wuhan, China). The following day, the samples were incubated in the dark at room temperature for 1 h with FITC-conjugated goat anti-rabbit IgG (1:500, ProteinTech, Wuhan, China). Nuclei were stained with DAPI (Beyotime, Beijing, China). Images were acquired using a laser scanning confocal microscope (Nikon, Japan) and analyzed using ImageJ software.

Flow cytometry

Macrophage surface biomarkers F4/80 and CD206 expression were analyzed by flow cytometry. The samples were incubated with anti-F4/80-Percp/cy5.5 (Biolegend, California, USA) and anti-CD206-PE (Biolegend, California, USA) for 30 min at 4 °C. Flow cytometric analysis was performed using a FACS Canto II (BD Biosciences, USA), and data were processed with FlowJo (version 10.7.1; BD Biosciences).

Apoptosis of MLE-12 cells was assessed using the Annexin V-FITC/PI Apoptosis Kit (Elabscience, Wuhan, China) according to the manufacturer's protocol. Apoptosis analysis was also conducted via flow cytometry using the FACS Canto II (BD Biosciences, USA).

Enzyme-linked immunosorbent assay (ELISA)

Mouse orbital venous plexus blood samples were centrifuged at 2500 rpm for 10 min at room temperature to obtain the serum [27]. Immunoglobulin E (IgE) levels in the serum were quantified using ELISA Kits (Ruixin Bio, Guangzhou, China). Additionally, the concentrations of IL-4, IL-5, IL-13, IL-10, TGF-β and IFN-γ in bronchoalveolar lavage fluid (BALF) were assessed using the same kit. The optical density (OD) at 450 nm was measured using a microplate reader (BIO-RAD, USA).

Statistical analysis

Statistical analysis was performed using GraphPad Prism 9 (La Jolla, CA). Data are presented as the mean ± SEM. Each experiment was conducted with at least three replicates. Statistical comparisons between two groups were made using the Student's t-test, while differences among multiple groups were assessed with one-way ANOVA. A P-value of < 0.05 was considered statistically significant.

Results

Characterization of M2Φ and M2Φ-Exos

Initial MH-S macrophages (M0Φ) were polarized into M2Φ by stimulation with IL-4, as described in previous studies [28, 29]. After 48 h of stimulation, morphological changes were observed under an optical microscope. M2Φ exhibited extended elongated morphology and pseudopodial [30, 31] (Fig. 1A). mRNA levels of M2-associated genes, including Arg1 ($P < 0.001$), MRC1 ($P < 0.001$) and Ym1 ($P < 0.05$), were significantly elevated (Fig. 1B-D). The mRNA levels of M1-associated genes, including TNF-α ($P < 0.01$), IL-1β ($P < 0.001$) and CD86 ($P < 0.05$) were decreased (Fig. 1E-G). Moreover, Flow cytometry analysis revealed significant upregulation of surface markers F4/80 and CD206 ($P < 0.001$) on IL-4–treated cells, indicative of M2Φ polarization (Fig. 1H).

Exosomes were isolated from the culture supernatant of M2Φ by differential ultracentrifugation (Fig. 1I). Transmission electron microscopy (TEM) and nanoparticle tracking analysis (NTA) were used to evaluate the morphology and size distribution of M2Φ-Exos. TEM

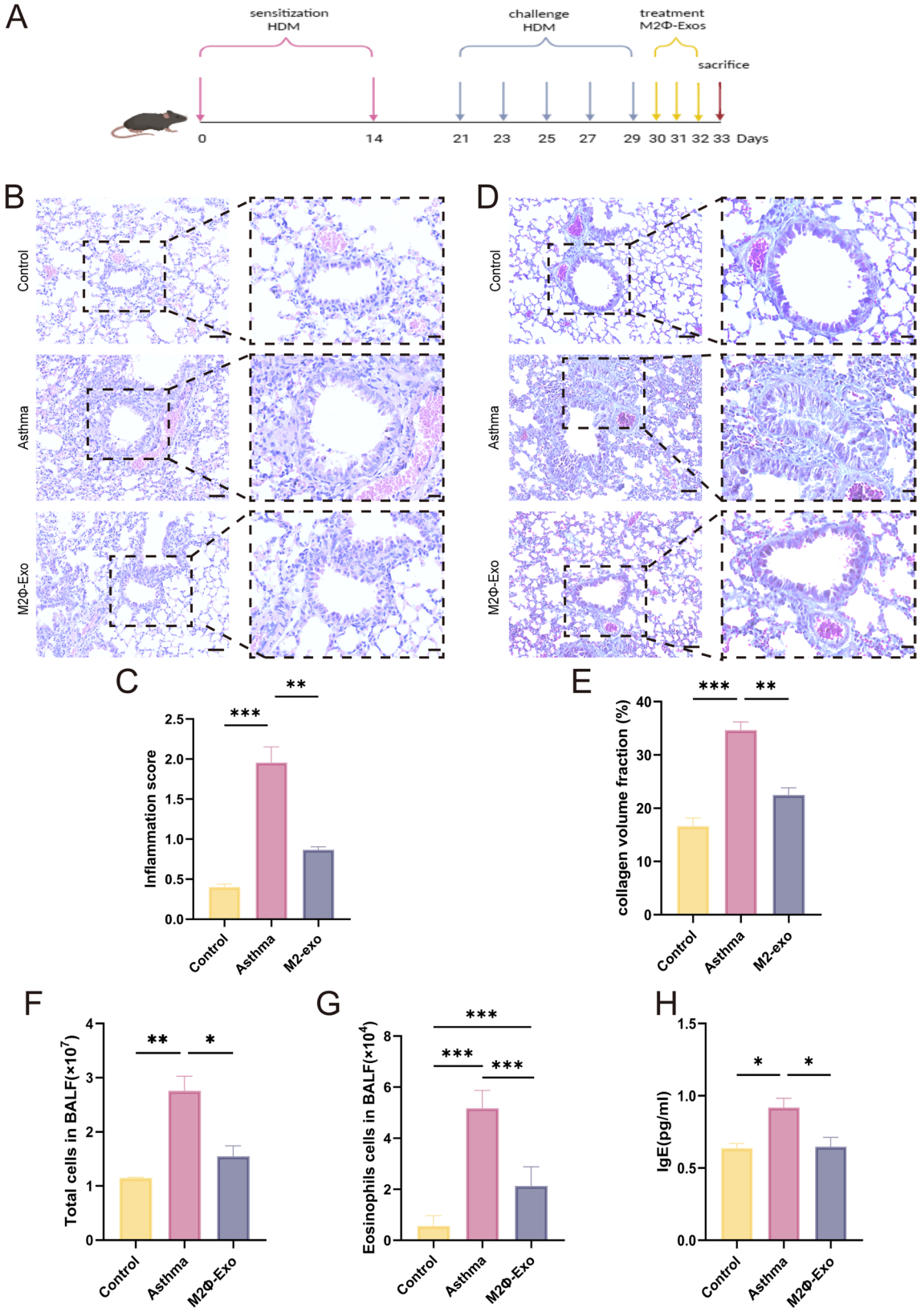

Fig. 4 (See legend on next page.)

(See figure on previous page.)

Fig. 4 M2Φ-Exosomes inhibit lung injury in HDM-induced asthmatic mice. **A** Schematic representation of the process used to establish the HDM-induced allergic asthma mouse model. M2Φ-Exosomes were administered intranasally as a reference treatment. **B** Representative H&E staining of lung tissue sections from the three experimental groups. Scale bars: 50 μm and 20 μm. **C** Lung inflammation scores in the mice across the different groups. **D** Collagen fibers in mouse lung tissues visualized by Masson's trichrome staining. Scale bars: 50 μm and 20 μm. **E** Quantification of collagen volume fraction. **F** Total cell count in the bronchoalveolar lavage fluid (BALF). **G** Eosinophil count in the BALF. **H** Total serum IgE levels in the mice, as analyzed by ELISA. *$P<0.05$, **$P<0.01$, ***$P<0.001$

imaging revealed a typical cup-shaped structure for the M2Φ-Exos (Fig. 1J), with a mean diameter of approximately 115.5 nm as determined by NTA (Fig. 1K). The presence of exosome markers CD9, TSG101, and CD63 was confirmed, while the endoplasmic reticulum marker calnexin was absent, supporting the identity of the isolated exosomes as M2Φ-derived (Fig. 1L).

M2Φ-Exos inhibit the abnormal proliferation of MLE-12 cells induced by HDM

PKH-26-labeled M2Φ-Exos were successfully internalized by MLE-12 cells (Fig. 2A). To identify the optimal treatment concentration, a CCK8 assay was conducted, revealing that M2Φ-Exos at a concentration of 80 μg/ml notably impacted cell viability ($P<0.01$) (Fig. 2B). Therefore, we chose 80 μg/ml for further experiments. Abnormal cell proliferation is a crucial element in airway remodeling associated with asthma [5]. Wound healing assays demonstrated that M2Φ-Exos inhibited cell migration in HDM-treated MLE-12 cells after 48 h ($P<0.05$) (Fig. 2C, D). Moreover, EdU incorporation assays showed a significant reduction in cell proliferation in the M2Φ-Exo-treated group compared to the HDM treatment group ($P<0.001$) (Fig. 2E, F). Immunofluorescence and Western blotting analyses revealed a decrease in PCNA expression in M2Φ-Exo-treated HDM-stimulated MLE-12 cells ($P<0.05$) (Fig. 2G-J). These results suggest that M2Φ-Exos play a role in regulating the abnormal proliferation of MLE-12 cells.

M2Φ-Exos reduce apoptosis in HDM-induced MLE-12 cells

Airway epithelial apoptosis plays a crucial role in both epithelial injury and the repair process [32]. To further explore the effects of M2Φ-Exos on apoptosis in HDM-treated MLE-12 cells, we utilized flow cytometry for apoptosis analysis. The results demonstrated that M2Φ-Exos significantly reduced HDM-induced apoptosis in MLE-12 cells ($P<0.001$) (Fig. 3A, B). Immunofluorescence staining for TUNEL further confirmed that apoptosis was markedly increased in the HDM-treated group compared to the control group ($P<0.001$), while M2Φ-Exos treatment notably reduced the number of apoptotic cells ($P<0.001$) (Fig. 3C, D). Additionally, the expression of Cleaved-caspase 3 was significantly lower in the M2Φ-Exos-treated group compared to the HDM-treated group, as evidenced by both immunofluorescence ($P<0.05$) (Fig. 3E, F) and Western blot analysis ($P<0.01$) (Fig. 3G-I). Furthermore, the M2Φ-Exos treatment group showed higher levels of the anti-apoptotic protein Bcl-2 ($P<0.05$) and lower levels of the pro-apoptotic protein Bax compared to the HDM-treated treatment group ($P<0.05$) (Fig. 3J-L). These findings suggest that M2Φ-Exos exert a protective effect by alleviating apoptosis in HDM-induced MLE-12 cells.

M2Φ-Exos attenuate lung injury in HDM-Induced asthmatic mice

To further investigate the effects of M2Φ-Exos in vivo, we developed an HDM-induced allergic asthma mouse model as shown in Fig. 4A. H&E staining of lung tissues revealed significant infiltration of inflammatory cells and thickening of the alveolar walls in the asthma group compared to the control group. However, these changes were notably diminished in the lung tissues of the M2Φ-Exo-treated asthmatic mice (Fig. 4B). The lung inflammation scores for each group are presented in Fig. 4C. Additionally, Masson'strichrome staining staining demonstrated that M2Φ-Exo treatment effectively reduced airway collagen fiber deposition and mitigated airway remodeling in asthmatic mice ($P<0.01$) (Fig. 4D, E). Furthermore, the M2Φ-Exo-treated groups exhibited significantly lower total cell counts ($P<0.05$) and eosinophil percentages ($P<0.001$) in the bronchoalveolar lavage fluid (BALF) compared to the asthma group (Fig. 4F, G). Moreover, IgE levels were significantly elevated in the asthma group but were reduced following M2Φ-Exo treatment in the HDM-induced asthma model ($P<0.05$) (Fig. 4H). These results suggest that M2Φ-Exos may alleviate lung injury in HDM-induced asthmatic mice.

M2Φ-Exos inhibit aberrant airway epithelial proliferation in asthmatic mice

We first examined the distribution of M2Φ-Exos in lung tissues. DiR-labeled M2Φ-Exos were administered intranasally to HDM-induced asthmatic mice. Fluorescence imaging revealed that M2Φ-Exos were localized within the lung tissues after 6 h (Fig. 5A, B). To further explore the effects of M2Φ-Exos on airway proliferation, we assessed PCNA expression in HDM-induced mice using Western blotting. The results showed a significant

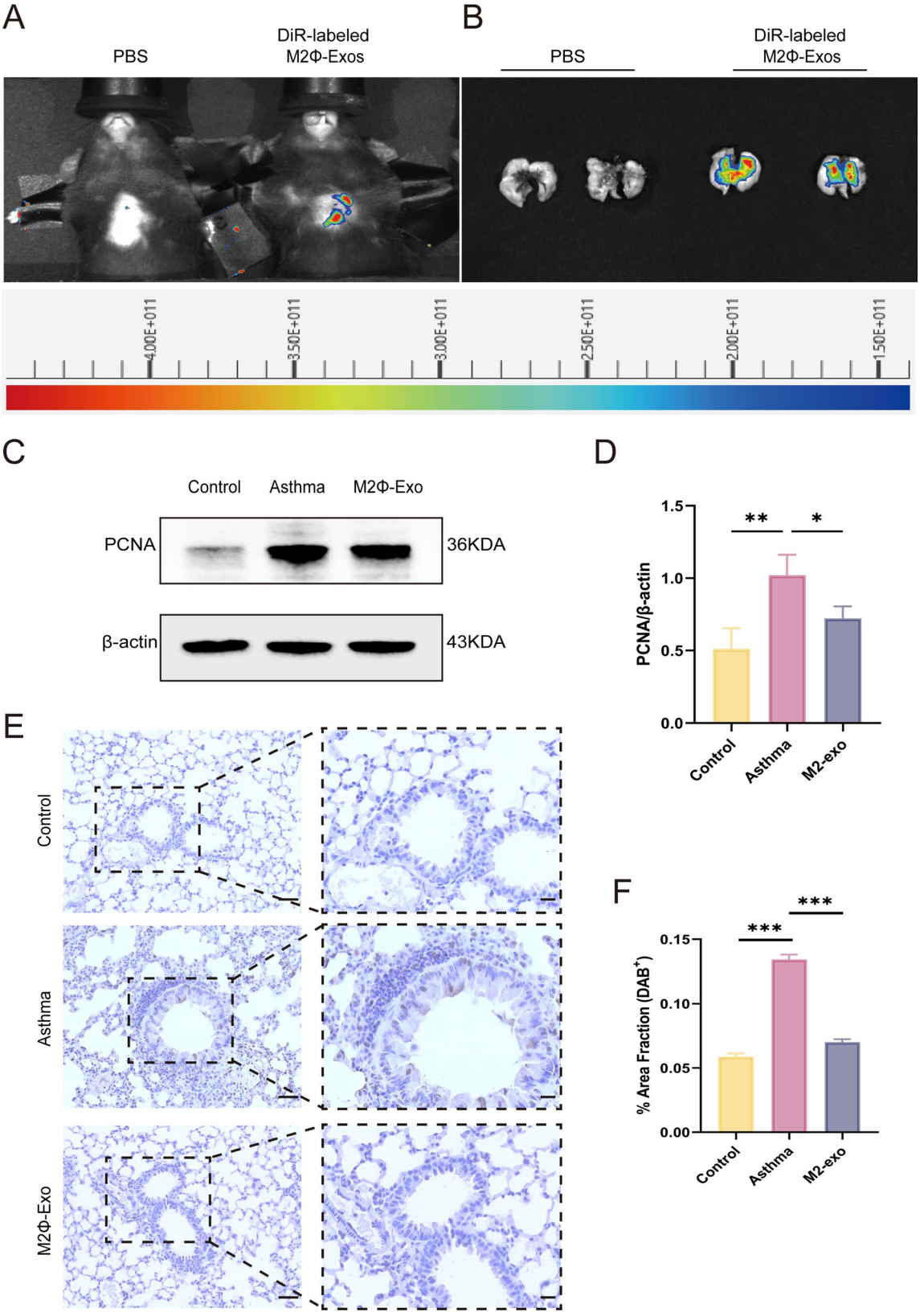

Fig. 5 (See legend on next page.)

(See figure on previous page.)

Fig. 5 M2Φ-Exosomes Inhibit Aberrant Airway Epithelial Cell Proliferation in Asthmatic Mice. **A** Intranasal administration of DiR-labeled M2Φ-Exosomes was detected via fluorescence imaging. **B** Localization of DiR-labeled M2Φ-Exosomes within lung tissues was observed using fluorescence imaging. **C** Representative Western blots showing PCNA protein levels in lung tissues. **D** Quantification of grayscale values of PCNA expression. **E** Immunohistochemical (IHC) staining of PCNA-positive proliferating cells in lung tissues. Scale bar: 50 μm and 20 μm. **F** Quantification of immunohistochemical staining. *$P < 0.05$, **$P < 0.01$

increase in PCNA levels following HDM treatment, which was reversed upon M2Φ-Exos administration ($P < 0.05$) (Fig. 5C, D). Additionally, immunohistochemical (IHC) staining of lung tissue from M2Φ-Exos-treated mice revealed fewer PCNA-positive proliferating cells compared to the asthma group ($P < 0.001$) (Fig. 5E, F). These findings suggest that M2Φ-Exos reduce aberrant epithelial cell proliferation in HDM-induced asthmatic mice.

M2Φ-Exos inhibit airway epithelial cell apoptosis in asthmatic mice

Studies have shown that aeroallergens increase apoptosis of epithelial cells, which aggravates airway epithelial barrier disruption and worsens asthma [13]. Therefore, we investigated the effect of M2Φ-Exos on airway epithelial cell apoptosis in asthmatic mice. Apoptosis in lung tissue was confirmed by TUNEL staining. The results demonstrated that cell apoptosis in the lung tissues of the M2Φ-Exos treatment group was lower than in the asthma group ($P < 0.01$) (Fig. 6A, B). Additionally, M2Φ-Exos treatment decreased Cleaved-caspase 3 expression in the lung tissues of HDM-induced asthmatic mice ($P < 0.05$) (Fig. 6C, D). Furthermore, the level of Cleaved-caspase 3 in M2Φ-Exos-treated mice was significantly lower compared to the asthma group ($P < 0.05$) (Fig. 6E, G). However, there was no statistically significant difference in Caspase 3 levels among the three groups ($P > 0.05$) (Fig. 6E, F). Bax protein levels were markedly decreased in the M2Φ-Exos treatment group compared to the asthma group ($P < 0.05$). Conversely, Bcl2 protein levels in the M2Φ-Exos treatment group were markedly higher than in the asthma group ($P < 0.05$) (Fig. 6H-J). IHC staining also revealed that Cleaved-caspase 3-positive cells were fewer in the M2Φ-Exos treatment group compared to the asthma group ($P < 0.001$) (Fig. 6K, L). Collectively, these results indicate that M2Φ-Exos reduce epithelial cell apoptosis in asthmatic mice.

M2Φ-Exos regulate inflammatory cytokines in asthmatic mice

Airway remodeling and inflammation are closely intertwined, perpetuating each other during asthma progression [33]. Epithelial damage triggers the release of cytokines such as IL-4 and IL-13, which further exacerbate epithelial injury, airway remodeling, and inflammatory infiltration, creating a vicious cycle. To investigate whether M2Φ-Exos influence the expression of inflammatory cytokines in the lungs and BALF of asthmatic mice, we conducted qRT-PCR and ELISA analyses.

Compared to the untreated asthma group, mice receiving M2Φ-Exos treatment exhibited significantly reduced mRNA expression levels of Th2 cytokines, including IL-4 ($P < 0.05$) (Fig. 7A), IL-5 ($P < 0.01$) (Fig. 7B), and IL-13 ($P < 0.05$) (Fig. 7C) and TGF-β ($P < 0.05$) (Fig. 7D), alongside increased levels of anti-inflammation cytokine IL-10 ($P < 0.05$) (Fig. 7E) and the Th1 cytokine IFN-γ (Fig. 7F) in lung tissue, as determined by qRT-PCR. Furthermore, ELISA results from BALF samples revealed a substantial reduction in IL-4 ($P < 0.01$), IL-5 ($P < 0.01$), IL-13 ($P < 0.01$) and TGF-β ($P < 0.001$) levels in the M2Φ-Exos treatment group compared to asthmatic controls (Fig. 7G-J). Notably, IL-10 ($P < 0.05$) (Fig. 7K) and IFN-γ ($P < 0.05$) (Fig. 7L) levels in BALF were significantly elevated following M2Φ-Exos administration.

These findings suggest that M2Φ-Exos may mitigate airway epithelial damage, thereby interrupting the cycle of airway inflammation and remodeling to some extent.

Discussion

The airway epithelium serves as the first line of defense against pathogens and allergens, acting as a crucial barrier while orchestrating immune responses [34]. Repeated injury to the airway epithelial cells and chronic inflammation disrupt epithelial homeostasis, leading to apoptosis and structural changes characteristic of airway remodeling [33]. These pathological changes are central to asthma's progression and highlight the need for novel therapeutic approaches targeting epithelial repair and inflammation.

In this study, we investigated the therapeutic potential of exosomes derived from M2 macrophages (M2Φ-Exos). M2 macrophages, known for secreting anti-inflammatory factors and tissue repair-associated proteins, present a promising avenue for therapeutic intervention in asthma and airway remodeling [35]. Exosomes are extracellular vesicles that have garnered considerable attention for their roles in immune regulation, tissue repair, and metabolic homeostasis in various diseases, including acute lung injury [36], atopic dermatitis [37], osteoarthritis [38], and cardiovascular conditions [39]. While

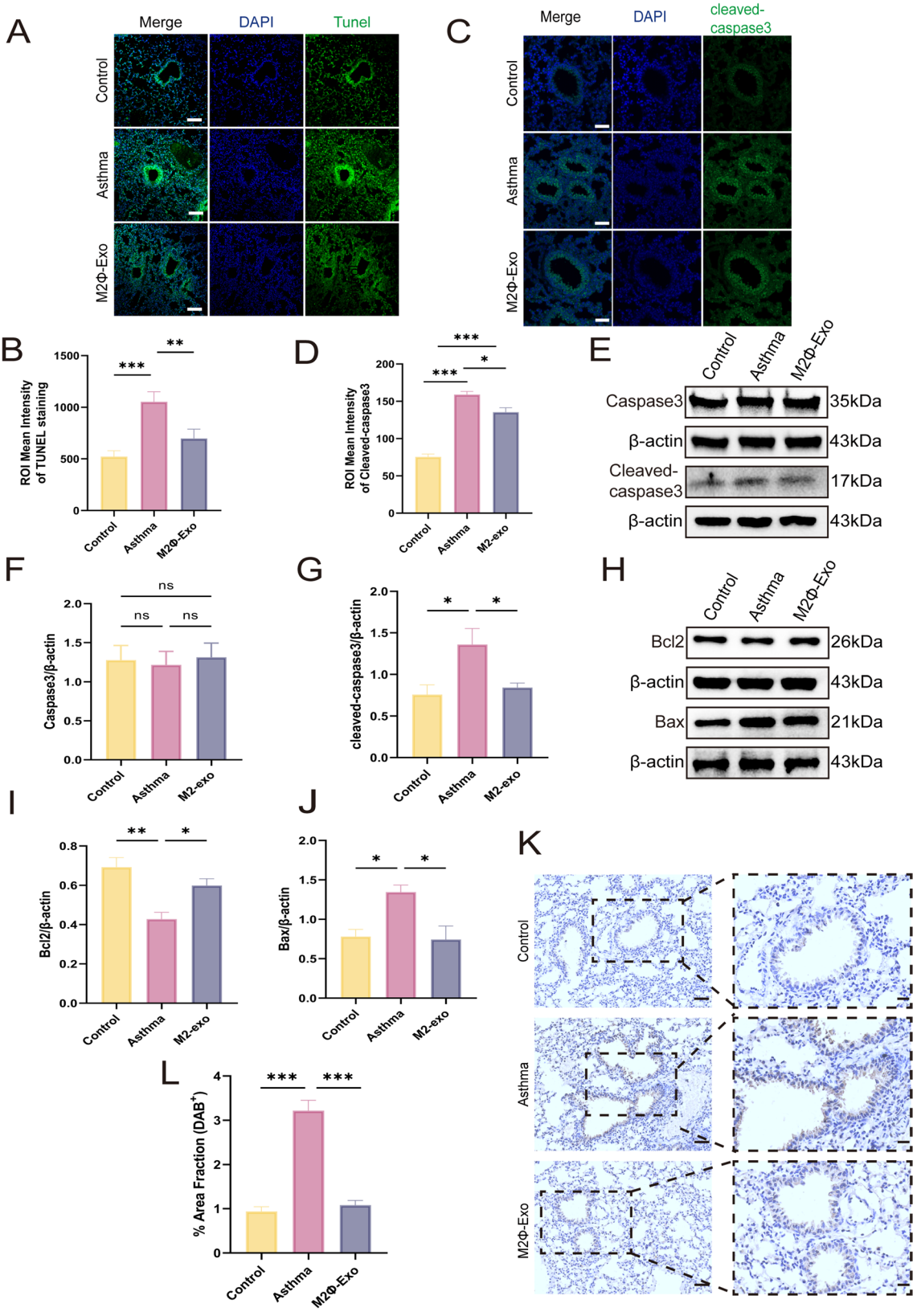

Fig. 6 (See legend on next page.)

(See figure on previous page.)

Fig. 6 M2Φ-Exosomes inhibit apoptosis of airway epithelial cells in asthmatic mice. **A** Representative images of TUNEL staining in lung tissue from asthmatic mice. Scale bar = 100 μm. **B** Quantification of the region of interest (ROI) mean intensity of TUNEL staining. **C** Immunofluorescence staining for Cleaved-caspase3 in lung tissue of mice. Scale bar = 50 μm. **D** Quantification of ROI mean intensity of Cleaved-caspase3. **E** Representative western blots showing caspase 3 and Cleaved-caspase3 protein expression. **F**, **G** Quantification of grayscale values for caspase 3 and Cleaved-caspase3. **H** Representative western blots of Bax and Bcl2 protein expression. **I**, **J** Quantification of grayscale values for Bax and Bcl2. **K** IHC staining for Cleaved-caspase3-positive cells in lung tissues. Scale bars = 50 μm and 20 μm. **L** Quantification of immunohistochemical staining. *$P < 0.05$, **$P < 0.01$, ***$P < 0.001$, ns, not significant

mesenchymal stem cell (MSC)-derived exosomes have been shown to suppress pulmonary inflammation and remodeling via pathways like Wnt/β-catenin [40], the specific contributions of macrophage-derived exosomes to lung diseases remain underexplored.

Using house dust mite (HDM)-induced MLE-12 cells and an HDM-induced asthmatic mouse model, we demonstrated that M2Φ-Exos regulate epithelial cell proliferation, apoptosis, and inflammation both in vitro and in vivo. In vitro, M2Φ-Exos co-cultured with HDM-induced MLE-12 cells reduced aberrant migration, hyperplasia, and apoptosis. In vivo, M2Φ-Exos mitigated alveolar thickening, restored Th1/Th2 cytokine balance, and alleviated epithelial apoptosis and inflammation. These findings suggest that M2Φ-Exos play a protective role in asthma by attenuating airway remodeling and immune dysregulation.

Exposure to allergens compromises the airway epithelial barrier, facilitating pathogen infiltration and exacerbating inflammation [5]. Persistent inflammation induces abnormal tissue repair, leading to airway remodeling and bronchial obstruction [41]. Dysfunctional airway epithelium in asthma is marked by weakened tight junctions and excessive proliferation—both key contributors to remodeling [7]. Our study revealed increased expression of proliferating cell nuclear antigen (PCNA), a pivotal regulator of DNA replication and repair, in HDM-induced MLE-12 cells and asthmatic mouse lung tissues. Notably, M2Φ-Exos treatment significantly reduced PCNA expression, supporting their role in modulating epithelial hyperplasia. Excessive proliferation is also linked to epithelial-mesenchymal transition (EMT), a process contributing to airway fibrosis and rigidity [42]. The observed reductions in epithelial hyperplasia may reflect the inhibition of EMT, underscoring the therapeutic potential of M2Φ-Exos in asthma management.

Apoptosis, while essential for normal epithelial turnover, contributes to pathological airway stiffening and narrowing in asthma. Corticosteroids, the mainstay of asthma treatment, may paradoxically exacerbate epithelial apoptosis and compromise barrier integrity without addressing the underlying disease processes [43]. Thus, there is a pressing need to identify therapeutic approaches that more effectively inhibit epithelial apoptosis. Our study confirmed heightened apoptosis in HDM-induced MLE-12 cells and lung tissues, which was significantly attenuated following M2Φ-Exos administration. These results highlight the capacity of M2Φ-Exos to modulate epithelial apoptosis, providing novel insights into strategies for airway remodeling and asthma management.

Epithelial apoptosis is further implicated in the overexpression of thymic stromal lymphopoietin (TSLP), an epithelial cytokine that drives Th2 differentiation and initiates Th2-dominated immune responses [44]. Asthma is characterized by an imbalance in Th1/Th2 cytokines, with elevated Th2 cytokines (IL-4, IL-5, IL-13) and suppressed Th1 cytokines (IFN-γ) contributing to airway inflammation and obstruction [45]. IL-10, an anti-inflammatory cytokine primarily secreted by regulatory T cells (Tregs), plays a crucial immunomodulatory role by suppressing IgE production and attenuating eosinophil infiltration in airways [46]. TGF-β plays critical roles in regulating key processes during lung development and maintaining pulmonary homeostasis. In asthma, TGF-β mediates both airway remodeling and immune modulation, critically influencing T cell development and airway immune homeostasis [47]. In our study, M2Φ-Exos effectively decreased IL-4, IL-5, IL-13 and TGF-β levels while increasing IL-10 and IFN-γ expression, consistent with their anti-inflammatory effects observed in other disease models. These findings underscore the ability of M2Φ-Exos to restore Th1/Th2 balance and mitigate airway inflammation.

Despite the promising therapeutic potential of M2Φ-Exos demonstrated in this study, the underlying mechanisms by which they regulate epithelial proliferation and apoptosis in asthma remain incompletely understood. Future research should focus on identifying the active components within M2Φ-Exos and elucidating their molecular targets. Additionally, optimizing the production and standardization of M2Φ-Exos will be critical for their translation into clinical applications. These steps will pave the way for innovative therapies targeting airway remodeling and inflammation in asthma.

In conclusion, our study revealed that the dysfunctional airway epithelium in asthma is characterized by an imbalance between abnormal proliferation and

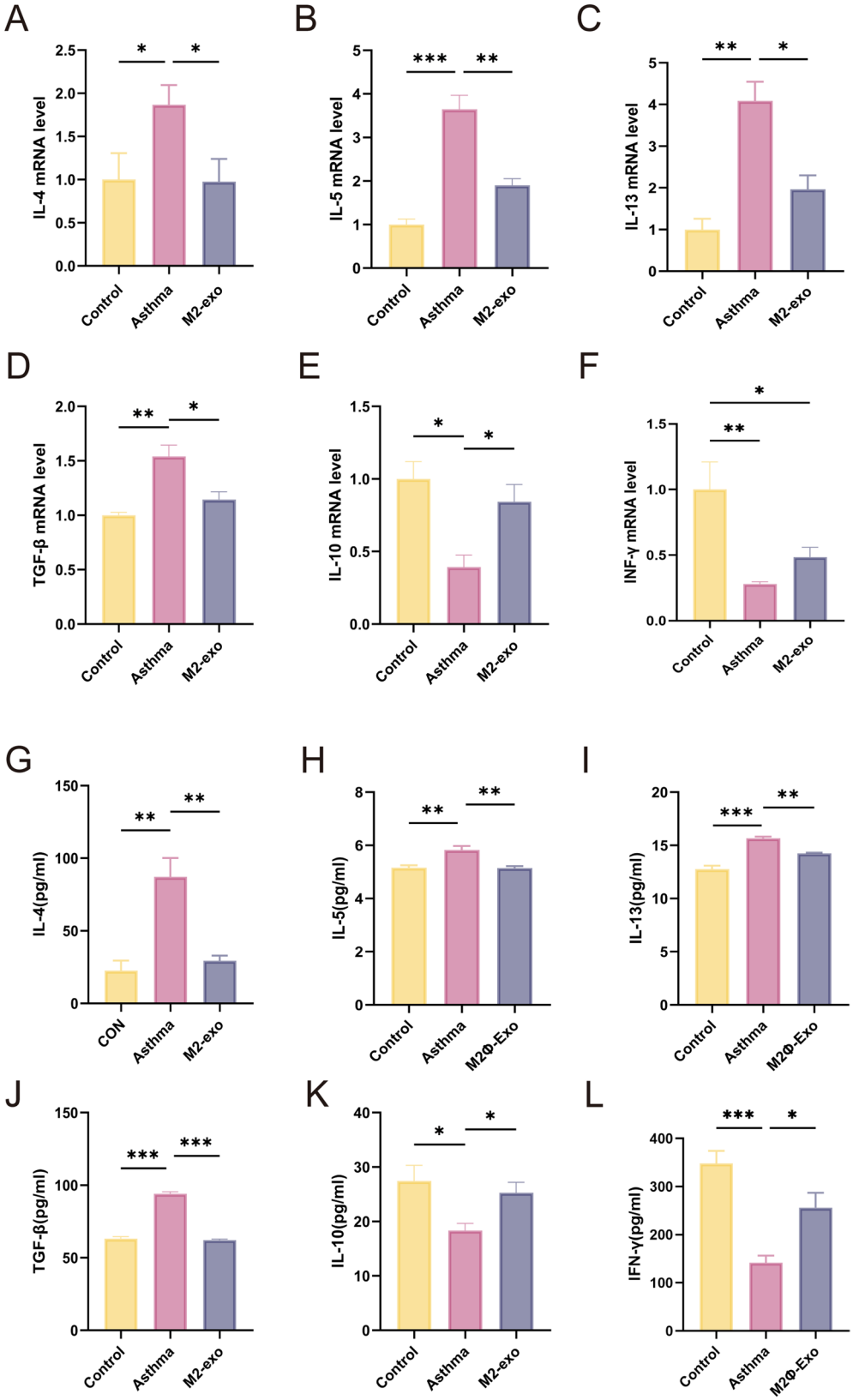

Fig. 7 M2Φ-Exosomes regulate inflammatory cytokines in asthmatic mice. Quantification of mRNA levels for (**A**) IL-4, (**B**) IL-5, (**C**) IL-13, (**D**) TGF-β, (**E**) IL-10 and (**F**) IFN-γ in lung tissue using qRT-PCR. Expression of (**G**) IL-4, (**H**) IL-5, (**I**) IL-13, (**J**) TGF-β, (**K**) IL-10 and (**L**) IFN-γ in BALF of mice detected by ELISA. $^{*}P < 0.05$, $^{**}P < 0.01$, $^{***}P < 0.001$

apoptosis. Notably, M2Φ-Exos demonstrated significant therapeutic potential by alleviating airway remodeling and inflammation, as well as regulating the proliferation and apoptosis in asthma. These findings provide new insights into the regulatory effects of M2-exosomes on the epithelial microenvironment in asthma and highlight their promise as a potential therapeutic strategy.

Abbreviations

M2Φ-ExosM2	Macrophage-derived exosomes
BALF	Bronchoalveolar lavage fluid
ICS	Inhaled corticosteroids
LABAs	Long-acting beta2-agonists
AECs	Airway epithelial cells
PCNA	Proliferating cell nuclear antigen
HDM	House dust mites
ROS	Reactive oxygen species
IACUC	Institutional animal care and use committee
NTA	Nanoparticle tracking analysis
TEM	Transmission electron microscopy
SPF	Specificpathogenfree
PBS	Phosphate-buffered saline
HE	Hematoxylin-eosin
IHC	Immunohistochemical
DAB	Diaminobenzidine
CCK-8	Cell counting kit-8
PVDF	Polyvinylidene fluoride
cDNA	Complementary DNA
ELISA	Enzyme-linked immunosorbent assay
IgE	Immunoglobulin E
TSLP	Thymic stromal lymphopoietin

Acknowledgements
None.

Authors' contributions
Y.Y.R., E.M.L., J.Y.Y., Z.X.L., Z.F., B.L. and F.X.D. were responsible for the overall conception and design of the study. Y.Y.R. performed most of the experiments and the data analysis, collected the data, and wrote the manuscript. Y.Y.R., B.L. and F.X.D. revising the manuscript. Y.Y.R, M.Z., Y.H.L., Y.L., J.Y.X. and F.D. contributed to the sample collection. All authors reviewed, edited and approved the manuscript.

Funding
This study was supported by the Science and Technology Research Program of Chongqing Municipal Education Commission (Grant No. KJQN202200419, KJQN202200411), Scientific Natural Science Foundation of Chongqing (Grant No. CSTB2022NSCQ-MSX0930, CSTC2020jcyj-msxmX0615), Project of China Postdoctoral Science Foundation (Grant No. 2022MD713713), Specially Funded Project of Chongqing Postdoctoral Science Foundation (Grant No. 2022CQBSHTB1009), Chongqing Medical Scientific Research Project (Joint Project of Chongqing Health Commission and Science and Technology Bureau) (Grant No. 2024QNXM026).

Data availability
The datasets used or analyzed during the current study are available from the corresponding author on reasonable request.

Declarations

Ethics approval and consent to participate
All experimental procedures were reviewed and approved by the Ethics Committee of the Children's Hospital of Chongqing Medical University (Approval Numbers: 0918001).

Consent for publication
Not applicable.

Competing interests
The authors declare no competing interests.

Author details
[1]Department of Respiratory Medicine, Ministry of Education Key Laboratory of Child Development and Disorders, National Clinical Research Center for Child Health and Disorders, China International Science and Technology Cooperation base of Child development and Critical Disorders, Chongqing Engineering Research Center of Stem Cell Therapy, Children's Hospital of Chongqing Medical University, No. 136, Zhongshan 2nd Road, Yuzhong Dis, Chongqing 400014, China
[2]Bristol Medical School, University of Bristol, Bristol, UK
[3]Great Ormond Street Institute of Child Health, University College London, London, UK
[4]Department of Cardiothoracic Surgery, Ministry of Education Key Laboratory of Child Development and Disorders, National Clinical Research Center for Child Health and Disorders, China International Science and Technology Cooperation base of Child development and Critical Disorders, Chongqing Engineering Research Center of Stem Cell Therapy, Children's Hospital of Chongqing Medical University, No. 136, Zhongshan 2nd Road, Yuzhong Dis, Chongqing 400014, China

Received: 5 February 2025 / Accepted: 12 May 2025
Published online: 19 May 2025

References

1. Shipp CL, Gergen PJ, Gern JE, Matsui EC, Guilbert TW. Asthma management in children. J Allergy Clin Immunol Pract. 2023;11:9–18.
2. Zhu C, Sun Y, Zhao Y, Hou J, Zhang Q, Wang P. Associations between children's asthma and allergic symptoms and phthalates in dust in metropolitan Tianjin, China. Chemosphere. 2022;302:134786.
3. Shin YH, Hwang J, Kwon R, Lee SW, Kim MS, Shin JI, Yon DK, GBD 2019 Allergic Disorders Collaborators. Global, regional, and National burden of allergic disorders and their risk factors in 204 countries and territories, from 1990 to 2019: a systematic analysis for the global burden of disease study 2019. Allergy. 2023;78:2232–54.
4. Zhou X, Zhang P, Tan H, Dong B, Jing Z, Wu H, Luo J, Zhang Y, Zhang J, Sun X. Progress in diagnosis and treatment of difficult-to-treat asthma in children. Ther Adv Respir Dis. 2023;17:17534666231213637.
5. Russell RJ, Boulet LP, Brightling CE, Pavord ID, Porsbjerg C, Dorscheid D, Sverrild A. The airway epithelium: an orchestrator of inflammation, a key structural barrier and a therapeutic target in severe asthma. Eur Respir J. 2024;63:2301397.
6. Noureddine N, Chalubinski M, Wawrzyniak P. The role of defective epithelial barriers in allergic lung disease and asthma development. J Asthma Allergy. 2022;15:487–504.
7. Inoue H, Akimoto K, Homma T, Tanaka A, Sagara H. Airway epithelial dysfunction in asthma: relevant to epidermal growth factor receptors and airway epithelial cells. J Clin Med. 2020;9:3698.
8. Haj-Salem I, Fakhfakh R, Bérubé JC, Jacques E, Plante S, Simard MJ, Bossé Y, Chakir J. MicroRNA-19a enhances proliferation of bronchial epithelial cells by targeting TGFβR2 gene in severe asthma. Allergy. 2015;70:212–9.
9. Vignola AM, Chiappara G, Siena L, Bruno A, Gagliardo R, Merendino AM, Polla BS, Arrigo AP, Bonsignore G, Bousquet J, Chanez P. Proliferation and activation of bronchial epithelial cells in corticosteroid-dependent asthma. J Allergy Clin Immunol. 2001;108:738–46.
10. Barros B, Almeida BR, Barros D, Toledo MS, Suzuki E. Respiratory epithelial cells: more than just a physical barrier to fungal infections. J Fungi (Basel). 2022;8:548.
11. Wang J, Sun H, Liu Y. The proliferative and anti-apoptosis functions of KGF/KGFR contributes to bronchial epithelial repair in asthma. Pulm Pharmacol Ther. 2020;63:101931.
12. James BN, Oyeniran C, Sturgill JL, Newton J, Martin RK, Bieberich E, Weigel C, Maczis MA, Palladino E, Lownik JC, et al. Ceramide in apoptosis and oxidative stress in allergic inflammation and asthma. J Allergy Clin Immunol. 2021;147:1936–e19489.
13. Song J, Wang J. SIRT3 regulates bronchial epithelium apoptosis and aggravates airway inflammation in asthma. Mol Med Rep. 2022;25:144.
14. Wang X, Berkowicz A, King K, Menta B, Gabrielli AP, Novikova L, Troutwine B, Pleen J, Wilkins HM, Swerdlow RH. Pharmacologic enrichment of exosome yields and mitochondrial cargo. Mitochondrion. 2022;64:136–44.

15. Soccio P, Moriondo G, Lacedonia D, Tondo P, Pescatore D, Quarato C, Carone M, Foschino Barbaro MP, Scioscia G. MiRNA and exosomal miRNA as new biomarkers useful to phenotyping severe asthma. Biomolecules. 2023;13:1542.
16. Cañas JA, Rodrigo-Muñoz JM, Gil-Martínez M, Sastre B, del Pozo V. Exosomes: a key piece in asthmatic inflammation. Int J Mol Sci. 2021;22:963.
17. Murray PJ. Macrophage polarization. Annu Rev Physiol. 2017;79:541–66.
18. Yunna C, Mengru H, Lei W, Weidong C. Macrophage M1/M2 polarization. Eur J Pharmacol. 2020;877:173090.
19. Peng Y, Zhou M, Yang H, Qu R, Qiu Y, Hao J, Bi H, Guo D. Regulatory mechanism of M1/M2 macrophage polarization in the development of autoimmune diseases. Mediators Inflamm. 2023;2023:8821610.
20. Wang Y, Lin Q, Zhang H, Wang S, Cui J, Hu Y, Liu J, Li M, Zhang K, Zhou F, et al. M2 macrophage-derived exosomes promote diabetic fracture healing by acting as an immunomodulator. Bioact Mater. 2023;28:273–83.
21. Wang Y, Mao J, Wang Y, Jiang N, Shi X. Multifunctional exosomes derived from M2 macrophages with enhanced odontogenesis, neurogenesis and angiogenesis for regenerative endodontic therapy: an in vitro and in vivo investigation. Biomedicines. 2024;12:441.
22. Jiao Y, Zhang T, Liu M, Zhou L, Qi M, Xie X, Shi X, Gu X, Ma Z. Exosomal PGE2 from M2 macrophages inhibits neutrophil recruitment and NET formation through lipid mediator class switching in sepsis. J Biomed Sci. 2023;30:62.
23. Zhang Y, Bi J, Huang J, Tang Y, Du S, Li P. Exosome: a review of its classification, isolation techniques, storage, diagnostic and targeted therapy applications. Int J Nanomed. 2020;15:6917–34.
24. Liu B, Hu D, Zhou Y, Yu Y, Shen L, Long C, Butnaru D, Timashev P, He D, Lin T, et al. Exosomes released by human umbilical cord mesenchymal stem cells protect against renal interstitial fibrosis through ROS-mediated P38MAPK/ERK signaling pathway. Am J Transl Res. 2020;12:4998–5014.
25. Li Y, Fu W, Xiang J, Ren Y, Li Y, Zhou M, Yu J, Luo Z, Liu E, Fu Z, et al. Long-chain acyl-CoA synthetase 4-mediated mitochondrial fatty acid metabolism and dendritic cell antigen presentation. Inflamm Res. 2024;73:819–39.
26. Li C, Deng C, Zhou T, Hu J, Dai B, Yi F, Tian N, Jiang L, Dong X, Zhu Q, et al. MicroRNA-370 carried by M2 macrophage-derived exosomes alleviates asthma progression through inhibiting the FGF1/MAPK/STAT1 axis. Int J Biol Sci. 2021;17:1795–807.
27. Xiang J, Liu B, Li Y, Ren Y, Li Y, Zhou M, Yu J, Luo Z, Liu E, Fu Z, Ding F. TFEB regulates dendritic cell antigen presentation to modulate immune balance in asthma. Respir Res. 2024;25:182.
28. Huang C, Du W, Ni Y, Lan G, Shi G. The effect of short-chain fatty acids on M2 macrophages polarization in vitro and in vivo. Clin Exp Immunol. 2022;207:53–64.
29. Yang J, Huang X, Yu Q, Wang S, Wen X, Bai S, Cao L, Zhang K, Zhang S, Wang X, et al. Extracellular vesicles derived from M2-like macrophages alleviate acute lung injury in a miR-709-mediated manner. J Extracell Vesicles. 2024;13:e12437.
30. Vogel DY, Glim JE, Stavenuiter AW, Breur M, Heijnen P, Amor S, Dijkstra CD, Beelen RH. Human macrophage polarization in vitro: maturation and activation methods compared. Immunobiology. 2014;219:695–703.
31. Sadofsky LR, Hayman YA, Vance J, Cervantes JL, Fraser SD, Wilkinson HN, Williamson JD, Hart SP, Morice AH. Characterisation of a new human alveolar Macrophage-Like cell line (Daisy). Lung. 2019;197:687–98.
32. Pu Y, Liu YQ, Zhou Y, Qi YF, Liao SP, Miao SK, Zhou LM, Wan LH. Dual role of RACK1 in airway epithelial mesenchymal transition and apoptosis. J Cell Mol Med. 2020;24:3656–68.
33. Banno A, Reddy AT, Lakshmi SP, Reddy RC. Bidirectional interaction of airway epithelial remodeling and inflammation in asthma. Clin Sci. 2020;134:1063–79.
34. Frey A, Lunding LP, Ehlers JC, Weckmann M, Zissler UM, Wegmann M. More than just a barrier: the immune functions of the airway epithelium in asthma pathogenesis. Front Immunol. 2020;11:761.
35. Pei W, Li X, Bi R, Zhang X, Zhong M, Yang H, Zhang Y, Lv K. Exosome membrane-modified M2 macrophages targeted nanomedicine: treatment for allergic asthma. J Control Release. 2021;338:253–67.
36. Xia L, Zhang C, Lv N, Liang Z, Ma T, Cheng H, Xia Y, Shi L. AdMSC-derived exosomes alleviate acute lung injury via transferring mitochondrial component to improve homeostasis of alveolar macrophages. Theranostics. 2022;12:2928–47.
37. Zhu T, Sun J, Ma L, Tian J. Plasma exosomes from children with atopic dermatitis May promote apoptosis of keratinocytes and secretion of inflammatory factors in vitro. Clin Cosmet Investig Dermatol. 2022;15:1909–17.
38. Wu Y, Li J, Zeng Y, Pu W, Mu X, Sun K, Peng Y, Shen B. Exosomes rewire the cartilage microenvironment in osteoarthritis: from intercellular communication to therapeutic strategies. Int J Oral Sci. 2022;14:40.
39. Nikdoust F, Pazoki M, Mohammadtaghizadeh M, Aghaali MK, Amrovani M. Exosomes: potential player in endothelial dysfunction in cardiovascular disease. Cardiovasc Toxicol. 2022;22:225–35.
40. Song J, Zhu XM, Wei QY. MSCs reduce airway remodeling in the lungs of asthmatic rats through the Wnt/β-catenin signaling pathway. Eur Rev Med Pharmacol Sci. 2020;24:11199–211.
41. Pain M, Bermudez O, Lacoste P, Royer PJ, Botturi K, Tissot A, Brouard S, Eickelberg O, Magnan A. Tissue remodelling in chronic bronchial diseases: from the epithelial to mesenchymal phenotype. Eur Respir Rev. 2014;23:118–30.
42. Liang Z, Zhang Y, Xu Y, Zhang X, Wang Y. Hesperidin inhibits tobacco smoke-induced pulmonary cell proliferation and EMT in mouse lung tissues via the p38 signaling pathway. Oncol Lett. 2023;25:30.
43. Dorscheid DR, Wojcik KR, Sun S, Marroquin B, White SR. Apoptosis of airway epithelial cells induced by corticosteroids. Am J Respir Crit Care Med. 2001;164:1939–47.
44. Murrison LB, Ren X, Preusse K, He H, Kroner J, Chen X, Jenkins S, Johansson E, Biagini JM, Weirauch MT, et al. TSLP disease-associated genetic variants combined with airway TSLP expression influence asthma risk. J Allergy Clin Immunol. 2022;149:79–88.
45. Ji T, Li H. T-helper cells and their cytokines in pathogenesis and treatment of asthma. Front Immunol. 2023;14:1149203.
46. Daneshvar-Ghahfarokhi S, Rahnama A, Mohammadi-Shahrokhi V. Teucrium polium extract attenuates inflammation in asthma by reducing RORgammat transcription and increasing IL-10 secretion in an ovalbumin-induced murine asthma model. Iran J Immunol. 2023;20:159–66.
47. Saito A, Horie M, Nagase T. TGF-beta signaling in lung health and disease. Int J Mol Sci. 2018;19:2460.

Publisher's Note